Journal of Ceramic Processing Research. Vol. 17, No. 3, pp. 253~256 (2016)

J O U R N A L O F
Ceramic Processing Research

Green upconversion luminescence of Yb^{3+}, Er^{3+} co-doped $NaLa(MoO_4)_2$ phosphors

Jeong Ho Ryu[a], Suk Hyun Kang[b] and Kwang Bo Shim[b,*]

[a]*Department of Materials Science and Engineering, Korea National University of Transportation, Chungbuk 380-702, Korea*
[b]*Division of Materials Science and Engineering, Hanyang University, Seoul 133-791, Korea*

The upconversion (UC) luminescence properties of polycrystalline Er^{3+}/Yb^{3+} co-doped $NaLa(MoO_4)_2$ phosphors synthesized by a simple solid-state reaction method were investigated in detail. Under 980 nm excitation, Er^{3+}/Yb^{3+} co-doped $NaLa(MoO_4)_2$ exhibited weak red emissions near 660 and670 nm, and strong green UC emissions at 530 and550 nm corresponding to the intra 4f transitions of Er^{3+} ($_4F_{9/2}$, $^2H_{11/2}$, $^4S_{3/2}$) → Er^{3+} ($_4I_{15/2}$). The optimum doping concentration of Er^{3+} and Yb^{3+} for highest emission intensity was determined by XRD and PL analysis. The Er^{3+}/Yb^{3+} (7.0/10.0 mol%) co-doped $NaLa(MoO_4)_2$ phosphor sample exhibited strongly shiny green emission. A possible UC mechanism for Er^{3+}/Yb^{3+} co-doped $NaLa(MoO_4)_2$ depending on the pump power dependence was discussed in detail.

Key words: Green upconversion, $NaLa(MoO_4)_2$, Two-photon process.

Introduction

Over the past several decades, rare earth (RE)-doped upconversion (UC) luminescence has received considerable attention because of their potential applications including three-dimensional displays [1], laser and optical amplifiers [2], solar cells [3, 4], and bio-technologies [5, 6]. Many RE ions have been researched as luminescent centers for UC materials. Among them, Er^{3+}-doped UC phosphors are very popular due to their abundant energy level for UC luminescence and high luminescent quenching concentration compared to other RE ions [7]. However, because Er^{3+} ions have a very low absorption cross-section of the $^4I_{11/2}$ level under 980 nm excitation, Er^{3+} single-doped UC phosphors have a relatively low emission intensity and pump efficiency. In order to overcome these drawbacks and enhance the UC emission efficiency, Yb^{3+} ions are generally used as co-dopant ions because they have a large absorption cross-section around 980 nm and a possible effective energy transfer from Yb^{3+} to the activator ions through the multi photon process [8,9].

The selection of the host matrix is another important factor to obtain highly efficient UC luminescence because the different crystal fields caused by structural symmetry of the host materials can contribute to inner shell transitions such as intra 4f-4f transitions in RE ions. Up to now, most of the RE-doped UC phosphors have been studied with halides [10], glasses [11] and chalcogenides [12]. However, they have poor chemical stabilities [13] and high production costs, restricting their practical application. Recently, metal oxide systems have been investigated as the host matrices for UC materials because they have very low excitation thresholds and are very chemically, mechanically, and thermally stable.

The scheelite structural $NaLa(MoO_4)_2$ has been investigated as a laser crystal because it exhibits a local disorder structure and a good physical-chemical stability [14]. The Mo^{6+} ions in $NaLa(MoO_4)_2$ matrix cause a strong crystal field because of their large electric charges and small radius. Consequently, the stark splitting of lanthanide ions in $NaLa(MoO_4)_2$ is enhanced, which will strengthen the energy transfer between ions [15]. Some lanthanide doped $NaLa(MoO_4)_2$ samples with micro and nano scale exhibited good luminescence properties [16]. Therefore, we expected that $NaLa(MoO_4)_2$ can be a good candidate for UC phosphor matrices. However, the UC luminescence of Er^{3+}/Yb^{3+} co-doped polycrystalline $NaLa(MoO_4)_2$ has not been studied extensively yet. Consequently, efficient optical conversion from near infrared (NIR) to visible UC emission in $NaLa(MoO_4)_2$ will have great impact on the various potential applications. In this work, Er^{3+}/Yb^{3+} co-doped $NaLa(MoO_4)_2$ were synthesized by a simple solid-state reaction method. Effects of Er^{3+}/Yb^{3+} concentration on crystal structure and UC emission properties were investigated in detail, and related possible UC mechanism was presented.

Experimental Procedure

Polycrystalline Er^{3+}/Yb^{3+} co-doped $NaLa(MoO_4)_2$ were synthesized by a simple solid-state reaction method. For the investigation of the UC luminescence with various Er^{3+}/Yb^{3+} concentrations, the molar ratios of the cations were varied as $NaLa_{1-x-y}(Er_x)(Yb_y)MoO_4$.

*Corresponding author:
Tel : +82-2-2290-0501
Fax: +82-2-2229
E-mail: kbshim@hanyang.ac.kr

The starting chemicals of Na_2CO_3 (Kojundo Chemicals, 99.99%), MoO_3 (Kojundo Chemicals, 99.99%), La_2O_3 (Kojundo Chemicals, 99.99%), Yb_2O_3 (Kojundo Chemicals, 99.99%) and Er_2O_3 (Kojundo Chemicals, 99.99%) were accurately weighted according to their stoichiometric amounts. The raw materials were ground thoroughly by ball-milling and heat-treated at 800 °C for 3 h in ambient atmosphere. The phase analysis was conducted using X-ray diffraction (XRD, Rigaku D/MAX2C, Japan, Cu-α (λ = 1.5046 Å)). Room-temperature UC luminescent spectra were obtained using a photoluminescence spectrophotometer (PerkinElmer, LS55 with an IR laser diode (980 nm, 100 mW)) in a range of 400-700 nm. The pump power dependence was calculated as the irradiation power from 20 to 110 mW (SPEX, 1404p, France)

Results and Discussion

Figure 1 shows the phase analysis of Er^{3+}/Yb^{3+} co-doped $NaLa(MoO_4)_2$ with (a) various Er^{3+} concentrations up to 15 mol% without Yb^{3+} and (b) various Yb^{3+} concentrations up to 15 mol% fixed at 7 mol% Er^{3+} calcined at 800 °C for 3 h by XRD. It can be seen that their diffraction patterns are in good agreement with the standard diffraction pattern of $NaLa(MoO_4)_2$ (JCPDS: No 24-1103). No impurities or secondary phases could be identified, which is evidence that single phase Er^{3+}/Yb^{3+} co-doped $NaLa(MoO_4)_2$ with

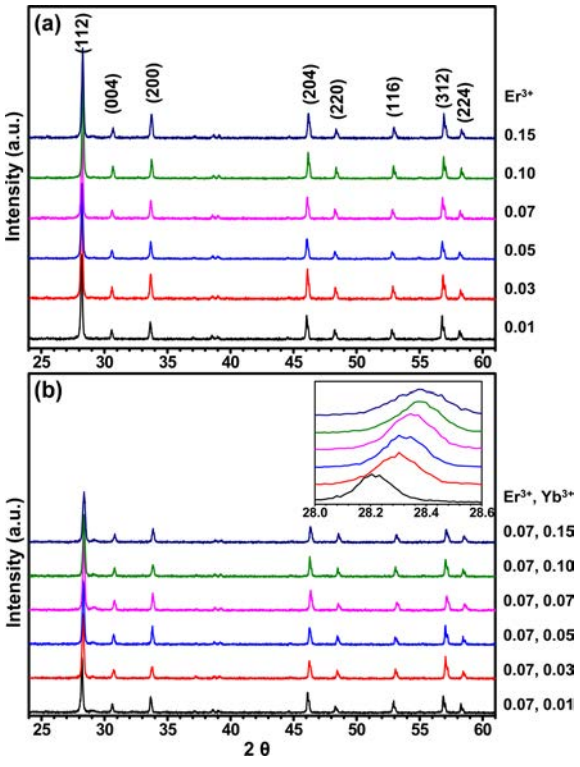

Fig. 1. X-ray diffraction patterns of Er^{3+}/Yb^{3+} co-doped $NaLa(MoO_4)_2$ UC phosphors with (a) Er^{3+} concentrations from 1.0 to 15.0 mol% and (b) Yb^{3+} concentrations from 1.0 to 15.0 mol% fixed at 7.0 mol% Er^{3+}. she inset of (b) represents that main diffraction peaks of (112) plane near 2θ = 28.3 ° shift to high angle with Yb^{3+} concentration.

Er^{3+} and Yb^{3+} concentrations up to 15 mol% can be obtained. These powders fundamentally maintained characteristics of scheelite structure, which are not affected by the doped lanthanide ions [17]. Based on the effective ionic radii of the cations with different coordination numbers (CN) [18] and large charge difference between La^{3+} ion and W^{6+} ion, it can be expected that Er^{3+} and Yb^{3+} [$r(Er^{3+})$ = 1.004 Å, $r(Yb^{3+})$ = 0.985 Å, when CN = 8] are preferably substituted into the La^{3+} sites [$r(La^{3+})$ = 1.16 Å, when CN = 8] instead of the W^{6+} sites [$r(W^{6+})$ = 0.66 Å, when CN = 4]. Note, that when the La^{3+} ions are substituted by the Er^{3+} or Yb^{3+} ions with smaller ionic radii than that of La^{3+}, the corresponding lattice constant becomes smaller. Therefore, as shown in the inset in Fig. 1(b), with higher Er^{3+}/Yb^{3+}concentrations, the diffraction peaks are shifted to a high 2θ angle, which illustrates that Er^{3+}/Yb^{3+} ions were well substituted into La^{3+} ion sites, resulting in reduction of lattice constants. Moreover, broadening of the diffraction peaks at (112) with increasing Er^{3+}/Yb^{3+} concentration shows that higher doping concentrations of the Er^{3+}/Yb^{3+} ions lead

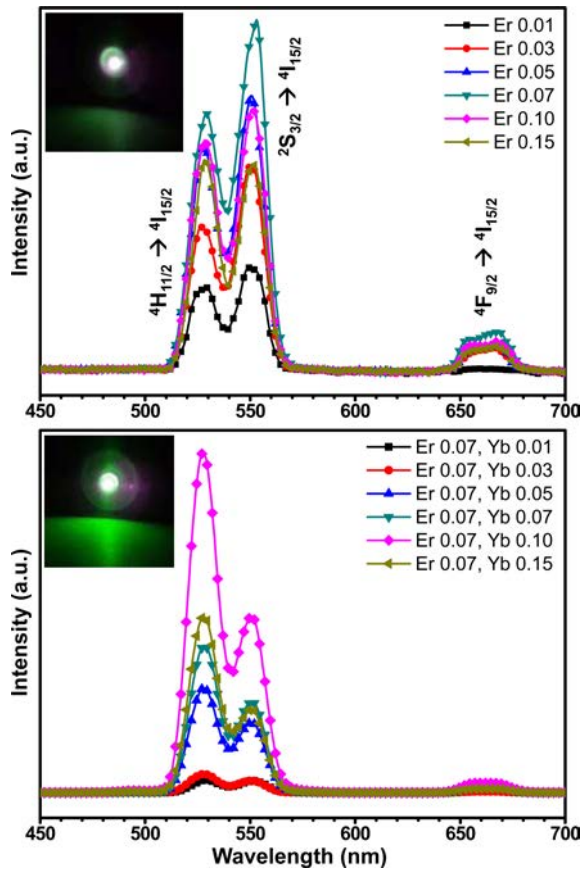

Fig. 2. Photoluminescent (PL) spectra of the Er^{3+}/Yb^{3+} co-doped $NaLa(MoO_4)_2$ UC phosphors with (a) Er^{3+} concentrations from 1.0 to 15.0 mol% and (b) Yb^{3+} concentrations from 1.0 to 15.0 mol% fixed at 7.0 mol% Er^{3+}. The photographs show Er^{3+} (7.0 mol%) doped and $Er^{3+/}Yb^{3+}$ (7.0/10.0 mol%) co-doped $NaLa(MoO_4)_2$ UC phosphor samples emit green light excited by a 980 IR laser (100 mW).

to decreased crystallinity.

Fig. 2 shows room temperature UC luminescent spectra of the Er^{3+}/Yb^{3+} co-doped $NaLa(MoO_4)_2$ (a) with Er^{3+} concentrations ranging from 1.0 to 15.0 mol% without Yb^{3+} and (b) Yb^{3+} concentrations ranging from 1.0 to 15.0 mol% fixed with 7.0 mol% Er^{3+} under excitation at 980 nm. The UC luminescent spectra of the Er^{3+}/Yb^{3+} co-doped $NaLa(MoO_4)_2$ consisted of three regions [19]: (1) intense green emissions near 530 nm assigned to the $^2H_{11/2} \rightarrow {}^4I_{15/2}$ transition, (2) near 550 nm attributed to the $^4S_{3/2} \rightarrow {}^4I_{15/2}$ transition, and (3) relatively weak red emission around 660 and 670 nm attributed to the $^4F_{9/2} \rightarrow {}^4I_{15/2}$ transition, which contribute to the intra 4f-4f transitions of Er^{3+} ions. All emission bands are accompanied by several well resolved Stark levels in Er^{3+}.

The concentration dependence of upconversion emissions could be mainly attributed to the interactions between doping ions. As seen in Fig. 2, the UC emission intensity of green emissions near 530 and 550 nm and red emissions around 656 and 670 nm increased with increasing Er^{+3} concentration from 1.0 to 7.0 mol% and with increasing Yb^{+3} concentration from 1.0 to 10.0 mol% then decreased beyond the optimum doping concentration due to the concentration quenching effect [20]. The concentration quenching effect can be explained by the energy transfer between nearest Er^{3+} and Yb^{3+} ions. That is, with increasing Er^{3+} and Yb^{3+} ion concentrations, the distance between Er^{3+} and Yb^{3+} ions will decrease, which can promote non-radiative energy transfer such as exchange interactions or multipole-multipole interactions [20]. Such a result is also observed from Er^{3+} doped or Er^{3+}/Yb^{3+} co-doped in other host matrices [21, 22]. Therefore, according to above mentioned results, the optimum Er^{3+}/Yb^{3+} doping concentration was found to be 7.0/10.0 mol%. The Er^{3+}/Yb^{3+} co-doped $NaLa(MoO_4)_2$ (7.0/10.0 mol%) specimen exhibited a strong green emission shiny to the naked eye when excited by a 980 nm laser diode (100 mW), as shown in inset of Fig. 2(b).

Fig. 3 shows the green and red UC luminescent emission intensities of Er^{3+}/Yb^{3+} co-doped $NaLa(MoO_4)_2$ (7.0/10.0 mol%) plotted on the logarithmic scale as a function of pump power. In the case of UC process, I is proportional to the exponent of P^n [21]. In this equation, n is the number of pumping photons required to excite the emitting state, I is the luminescent intensity, and P is the laser pumping power. The calculated n values are 1.73 and 1.62, for green emissions at 530 and 550 nm, and 1.63 for emissions at 660 and 670 nm, respectively. The n values for green emission at 530 nm ($^4I_{11/2} \rightarrow {}^4I_{15/2}$), 550 nm ($^4S_{3/2} \rightarrow {}^4I_{15/2}$) and for red emission at 660 nm and 670 nm ($^4F_{9/2} \rightarrow {}^4I_{15/2}$) are close to 2, which are in good agreement with previous n values obtained for green and red emissions in Er^{3+} ions [22]. These results indicate that the UC mechanism corresponding to green and red emissions occurs via a two-photon process.

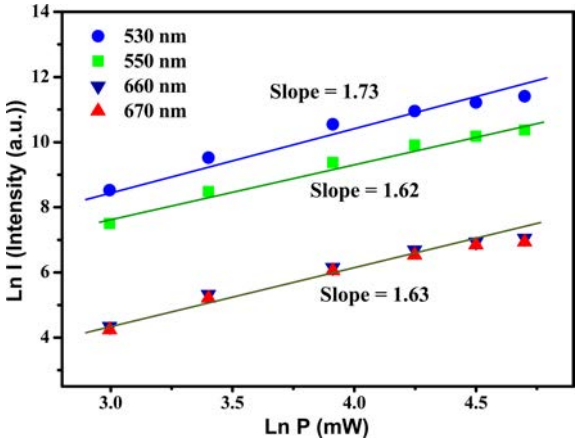

Fig. 3. Power dependence of the UC emission intensities of the Er^{3+}/Yb^{3+} (7.0/10.0 mol%) co-doped $NaLa(MoO_4)_2$ UC phosphor sample at 530, 550, 660 and 670 nm, respectively.

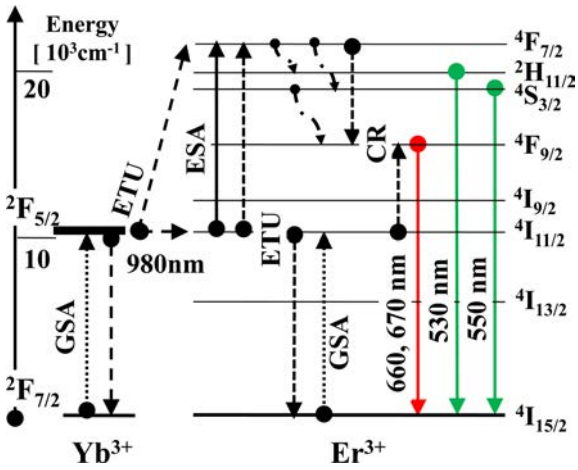

Fig. 4. Energy level diagram of Er^{3+} and Yb^{3+} in the $NaLa(MoO_4)_2$ crystal and possible UC mechanism under excitation at 980 nm.

To better comprehend the mechanism which populates the green ($^2H_{11/2}$, $^4S_{3/2} \rightarrow {}^4I_{15/2}$) and red ($^4F_{9/2} \rightarrow {}^4I_{15/2}$) luminescence, the UC emission mechanism and population processes for the Er^{3+}/Yb^{3+} co-doped $NaLa(MoO_4)_2$ system are schematically illustrated in Fig. 4. Under excitation at 980 nm, Er^{3+} and Yb^{3+} ions are initially excited from the ground state to the excited state through the ground state absorption (GSA) process (Er^{3+}: $^4I_{15/2} \rightarrow {}^4I_{11/2}$,$Yb^{3+}$: $^2F_{7/2} \rightarrow {}^2F_{5/2}$) or the energy transfer (ET) process of $^2F_{5/2}(Yb^{3+}) + {}^4I_{15/2}(Er^{3+}) \rightarrow {}^2F_{7/2}(Yb^{3+}) + {}^4I_{11/2}(Er^{3+})$ are responsible for the population at the $^4I_{11/2}$ level in Er^{3+}. For the green emissions, there are three possible processes for the energy transition from the $^4I^{11/2}$ level to the $^4F_{7/2}$ level of Er^{3+}, as follows [23-25].

(1) ESA: $^4I_{11/2}$ + a photon (980 nm) $\rightarrow {}^4F_{7/2}$
(2) ET: $^2F_{5/2}(Yb^{3+}) + {}^4I_{11/2}(Er^{3+}) \rightarrow {}^2F_{7/2}(Yb^{3+}) + {}^4F_{7}2(Er^{3+})$
(3) ET: $^4I_{11/2}(Er^{3+}) + {}^4I_{11/2}(Er^{3+}) \rightarrow {}^4F_{7/2}(Er^{3+}) + {}^4I_{15/2}(Er^{3+})$

These three possible processes populate from the $^4I_{11/2}$ level to the $^4F_{7/2}$ level in the Er^{3+} level, and then the $^4F_{7/2}$ level relaxes rapidly and non-radiatively to the next lower levels at $^2H_{11/2}$ and $^4S_{3/2}$ in Er^{3+} because of short lifetime of the $^4F_{7/2}$ level [26]. As a result, the above processes can produce green emissions in the spectral lines near 530 and 550 nm through the radiative transitions of $^2H_{11/2}/^4S_{3/2} \rightarrow {}^4I_{15/2}$. For the red emission, the $^4F_{9/2}$ level is generated by non-radiative relaxation from the $^4S_{3/2}$ to the $^4F_{9/2}$ level and cross relaxation (CR) via the $^4F_{7/2} + {}^4I^{11/2} \rightarrow {}^4F_{9/2} + {}^4F_{9/2}$ transition in Er^{3+} [27]. Finally, the $^4F_{9/2}$ level relaxes radiatively to the ground state at the $^4I_{15/2}$ level and releases red emission at 660 and 670 nm, as shown in Fig. 2(a,b). The UC emission is dominated to strong green emission at 530 ($^2H_{11/2} \rightarrow {}^4I_{15/2}$) and 550 nm ($^4S_{3/2} \rightarrow {}^4I_{15/2}$). The red emissions are very weak due to the weak absorption cross-section of the $^4I_{13/2}$ level [28]. Moreover, as the Er^{3+} and Yb^{3+} concentration increases up to 7.0/10.0 mol%, the green UC emission dramatically increases compared to the red emission. This is possibly due to the probability of electrons in the $^4I_{11/2}$ level being populated to the $^4F^{7/2}$ level via the energy transfer UC (ETU) process, which is much higher than that of non-radiative relaxation to the $^4I_{13/2}$ level [28].

Moreover, it is worth noting that $NaLa(MoO_4)_2$ can be a great candidate for green UC phosphors and would play important roles in the industrial fields that need green UC phosphors because green emitting property of the Er^{3+}/Yb^{3+} co-doped $NaLa(MoO_4)_2$ does not change with Yb^{3+} concentration, while UC emission color of Y_2O_3-like representative oxide UC phosphors change from green to red emission as Yb^{3+} doping concentrations [29].

Summary

Er^{3+}/Yb^{3+} co-doped $NaLa(MoO_4)_2$ UC phosphors were synthesized by a simple solid-state reaction method. Under NIR excitation (980 nm), Er^{3+}/Yb^{3+} co-doped $NaLa(MoO_4)_2$ phosphors exhibited obviously bright green UC luminescence at 530 and 550 nm with weak red emission at 660 and 670 nm. It was found that the UC emission intensity depends on Yb^{3+} acting as a sensitizer ion to improve the absorption cross-section around 980 nm, while Er^{3+} acts as an activator ion for UC luminescent centers in the $NaLa(MoO_4)_2$ matrix. The optimum doping concentrations of Er^{3+} and Yb^{3+} for highest green UC luminescence were 7.0 and 10.0 mol%, respectively. The UC emission is dominated by strong green emissions at 530 and 550 nm compared to red emissions at 660 and 670 nm which are resulted from the weak absorption cross-section of the $^4I_{13/2}$ level in Er^{3+} and the probability that electrons in the $^4I_{11/2}$ level get populated to the $^4F_{7/2}$ level via the ETU process, which is much higher than that of non-radiative relaxation to the $^4I_{13/2}$ level. Moreover, a two-photon process is responsible for both the UC green luminescence generated by $^2H_{11/2}$, $^4S_{3/2} \rightarrow {}^4I_{15/2}$ and the red emission generated by $^2F_{7/2} \rightarrow {}^4I_{15/2}$ in Er^{3+}/Yb^{3+} co-doped $NaLa(MoO_4)_2$ phosphors. Therefore, based on our results, it was concluded that Er^{3+}/Yb^{3+} co-doped $NaLa(MoO_4)_2$ can be an excellent candidate for green UC phosphors.

References

1. J. Mendez-Ramos, V. K. Tikhomirov, V. D. Rodriguez and D. Furniss, J. Alloy.Compd. 440 (2007) 328-335.
2. J. H. Zhang, H. Z. Tao, Y. Chang and X. J. Zhao, J. Rare. Earth 25 (2007) 108-120.
3. T. Trupke, M. A. Green and P. Würfel, J. Appl. Phys. 92 (2002) 4117-4220.
4. B. S. Richards and A. Shalav, IEEE Trans. Electron Devices 54 (2007) 4117-4222.
5. E. Downing, L. Hesselink, J. Ralston and R. Macfarlane, Science 273 (1996) 1185.
6. A. Rapaport, J. Milliez, M. Bass, A. Cassanho and H. Jenssen, J. Disp. Technol. 2 (2006) 68-70.
7. X. Li, J. Y. Wang and J. Li, J. Lumin. 12 (2007) 351-353.
8. H. X. Yang, H. Lin, Y. Y. Zhang, B. Zhai and E. Y. B. Pun, J. Alloy. Compd. 453 (2008) 493-498.
9. M. Liu, S. W. Wang, J. Zhang, L. Q. An and L. D. Chen, Opt. Mater. 29 (2007) 1352-1355.
10. J. C. Boyer, F. Vetrone, L. A. Cuccia and J. A. Capobianco, J. Am. Chem. Soc. 128 (2006) 1352-1355.
11. J. J. Owen, A. K. Cheetham and R. A. McFarlane, J. Opt. Soc. Am. B, 15 (1998) 684-688.
12. A. S. Oliveria, M. T. de Araujo and A. S. Gouveia, Appl. Phys. Lett. 72 (1998) 753-757.
13. S. K. Singh, K. Kumar and S. B. Rai, Sensors Actuators A: Phys. 149 (2009) 16-22.
14. M. Rico, J. Liu, J. M. Cano-Torres, A. Grarcia-Cortes, C. Cascales, C. Zaldo, U. Griebner and V. Petrov, Appl. Phys. B, 81 (2005) 621-625.
15. L. H. C. Andrade, M. S. Li, Y. Guyot, A. Brenier and G. Boulon, J. Phys.: Condens. Matter. 18 (2006) 7883-7888.
16. Z. Fu, W. Xia, Q. Li, X. Cui and W. Li, CrystEngComm, 14 (2012) 4618-4622.
17. J. Liu, H. Lian and C. Shi, Opt. Mater. 29 (2007) 1591-1595.
18. R. D. Shannon, Acta Cryst. A 32 (1976), 751-755.
19. X. -X. Luo and W. -H. Cao, J. Mater. Res. 23 (2008) 2078-2088.
20. D. Yang, C. Li, G. Li, M. Shang, X. Kang and J. Lin, J. Mater. Chem. 21 (2011), 5923-5928.
21. H. Guo, N. Dong, M. Yin, W. Zhang, L. Lou and S. Xia, J. Phys. Chem. B 108 (2004), 19205-19209.
22. Y. Bai, K. Yang, Y. Wang, X. Zhang and Y. Song, Opt. Comm. 281 (2008) 2930-2940.
23. F. Auzel, Chem. Rev. 104 (2004) 139-149.
24. F. Wang and X. Liu, Chem. Soc. Rev. 38 (2009) 976-980.
25. G. Y. Chen, H. C. Liu, H. J. Liang, G. Somesfalean and Z. G. Zhang, Solid State Commun. 196 (2008) 148-155.
26. V. Singh, V. K. Rai, K. A. Shamery, J. Nordmann and M. Haase, J. Lumin. 131 (2011) 2679-2689.
27. Q. Sun, X. Chen, Z. Liu, F. Wang, Z. Jiang and C. Wang, J. Alloy. Compd. 509 (2011) 5336.
28. S. Das, A. A. Reddy and G. V. Prakash, Chem. Phys. Lett. 504 (2011) 206.
29. H. Song, B. sun, T. Wang, S. Lu, L. Yang, B. Chen, X. Wang and X. Kong, Solid State Commun. 132 (2004) 409.